Uncertainty propagation in locally damped dynamic systems

L. Cortes, N. S. Ferguson and A. Bhaskar
Institute of Sound and Vibration Research
University of Southampton, SO17 1BJ Southampton, United Kingdom,
e-mail: **L.Cortes-Mochales@soton.ac.uk**

Abstract

In the field of stochastic structural dynamics, perturbation methods are widely used to estimate the response statistics of uncertain systems. When large built up systems are to be modelled in the mid-frequency range, perturbation methods are often combined with finite element model reduction techniques in order to considerably reduce the computation time of the response. Existing methods based on Component Mode Synthesis (CMS) allow the uncertainties in the system parameters to be treated independently in each of the substructures and the perturbation in the local parameters to be propagated to the full system global parameters. However, local treatment of damping uncertainty is usually avoided by assuming proportional damping. Here, a perturbation method that includes local modal damping uncertainty and its propagation to the global response is proposed. Local damping is accounted for in the CMS model by use of complex modes. A perturbation relationship between local and global modal properties is stated for non-classically damped systems. In this way, the response statistics for uncertain systems with localized damping can be computed at a low computational cost. A numerical example is presented to illustrate the performance of the proposed method.

1 Introduction

In the design stage of mechanical structures computer-aided engineering (CAE) methodologies are used for modelling the behaviour of the structures and optimising their performance. The vibrations of dynamic structures are often analysed using the finite element (FE) method. For large built-up structures the FE analysis computational cost raises dramatically as the analysis frequency increases. This happens because the FE mesh has to be further refined to account for small wavelengths corresponding to high frequency modes. Hence, modelling of large built-up structures is commonly addressed using finite element substructuring and model reduction techniques like component mode synthesis (CMS), in order to considerably reduce computation time.

Nevertheless, the high computational cost due to FE meshing requirements is not the only issue to be faced when the analysis frequency increases. An FE model of a mechanical structure is characterized through its physical parameters e.g. density, dimensions, Young's modulus, etc. It is therefore a deterministic model defined by certain nominal values of the parameters. In real structures, however, it is impossible to know with infinite precision the value of those physical parameters. Moreover, the parameter values might be slightly different for each instance of a manufactured structure. At low frequencies these tiny variations/errors in the parameters do not produce significant errors in the FE solution. However, when the FE analysis frequency increases, the modal frequencies and mode shapes become very sensitive to small variation in the parameter values. This might give rise to major errors in the computed FE response. Consequently, at mid-frequencies there is the need to account for the uncertainties in the physical parameters in order to compute robust estimates of the response of a system. The so called mid-frequency range is the frequency range in which uncertainties become significant but, yet, statistical methods, such as statistical energy analysis (SEA), do

not give accurate results due to the lack of modal density and modal overlap.

Stochastic Finite Element Method (SFEM) is the generic name given to the methods that introduce uncertainties in an FE model and seek to compute not only the nominal response of the system but also its statistics (mean responses, variances, covariances, confidence levels, etc). These SFEM methods involve the use of Monte Carlo (MC) methods. That is, computing the system response for a large amount of slightly different FE parameters sets, usually named Monte Carlo samples. As stated above, Conducting a single FE analysis at mid-frequencies has a high computational cost, notwithstanding if FE analyses are to be run for a large amount of MC samples. The required computational time then becomes impracticable. For this reason, SFEM methods usually solve the nominal model once and then make use of approximations in order to compute the rest of MC samples at a lower computational cost.

In this context, component mode synthesis has been identified to be a suitable framework for the quantification and propagation of uncertainties [1]. On one hand CMS allows the uncertainties in the system parameters to be treated independently in each of the substructures. This is convenient in many cases since it is likely that the different parts of built up structures have distinct uncertain nature. On the other hand, the use of perturbation methods on the CMS parameters makes it possible to drastically reduce the computational effort of the Monte Carlo simulations. Nevertheless, existing CMS perturbation techniques avoid the local treatment of damping by assuming proportional damping. When designing dynamic structures, however, damping is usually added in localized zones in order to reduce their noise and vibration levels. Therefore, the proportional damping assumption appears to be quite inaccurate in these cases.

This paper presents a perturbation method for SFEM based on complex component mode synthesis. The main feature of this method is that complex modes are used for the CMS component modal basis. In this way, damping and damping perturbations can be addressed at the component level. Then, perturbations in the component parameters are propagated into full system modal parameters through a first order approximation sensitivity relationship, so that the statistics of the frequency response functions for systems with localized damping can be computed at a low computational cost.

2 Component mode synthesis, perturbations and damping

Component mode synthesis was introduced in the 1960's by Hurty [2] and Craig and Bampton [3] and it is nowadays a well established sub-structuring technique. Classical CMS methods are defined for undamped systems, where the structure is divided into several components and their undamped free/fixed interface modes are computed. Model reduction is obtained by truncating the series of undamped component modes. Damping is assumed to be proportional and therefore it is introduced directly into the global modes once the full structure undamped solution has been computed.

In uncertainty analysis, perturbation approaches have been often used together with component mode synthesis [1, 4, 5]. In 1968 Fox and Kapoor [6] derived first and second order expressions for the rate of change of modal frequencies and mode shapes due to perturbation in physical parameters. Based on Fox and Kapoor, Mace and Shorter developed the local modal perturbational (LMP) method [4] in which the mass and stiffness matrices expressed in fixed interface Craig-Bampton coordinates were introduced into the Fox and Kapoor linear expressions. In this way they derived a simple sensitivity expression relating the perturbations in component modes to the global modal frequencies and mode shapes. In this and other methods classical CMS formulation is used, which implies that damping is not introduced at a component level.

Over the last decades, however, other CMS methods have been developed so that non-proportional damping can be included at a component modal level. For example, Craig and Ni [7] developed the inertia-relief attachment modes method based on a first order state-space formulation. Wang and Kirkhope [8] extended the method using complex modes and complex coupling interfaces, naming it complex component mode synthesis. More recently Morgan et al. [9] derived an alternative formulation using also complex modes that is a direct extension to the non-proportionally damped case of the classical Craig-Bampton methods. Thus,

it should be possible to develop new perturbation based methods that include non-proportional damping formulation. Indeed, Fox and Kapoor's linear expressions were extended to the non-proportional viscous damping case by Adhikari [10] some years ago. However, these expressions are not directly applicable to CMS formulation.

Recently, Ouisse et al. [11] presented a robust CMS method for the optimization of stochastic damped systems. In their work they work out an ad-hoc formulation for the fluid-structure coupling case. The Ritz basis is enriched with static residuals associated with visco-elastic and poro-elastic behaviour, and with the static response of residual forces due to structural modifications.

The purpose of this paper is to present an alternative method that is able to perform uncertainty analysis based on perturbations using the CMS formulation that includes damping at a component level. The main idea is to extend the LMP method for non-classically damped cases. This is done in a straightforward manner by use of complex component mode synthesis.

3 Component mode synthesis

Component mode synthesis is a method to solve in an efficient way the finite element model of a system. CMS performs modal analysis for the undamped system, and modal damping is later introduced into the undamped modes. From the equations of motion of an undamped system

$$\boldsymbol{M}\ddot{\boldsymbol{u}} + \boldsymbol{K}\boldsymbol{u} = \boldsymbol{f} \tag{1}$$

the modal parameters can be computed by solving the eigenvalue problem (EVP) for the homogeneous equations of motion

$$\boldsymbol{K}\phi = \lambda \boldsymbol{M}\phi \tag{2}$$

where λ and ϕ are the eigenvalue and eigenvector solutions respectively. Each solution of the EVP is an undamped mode m of vibration, with ϕ_m being its mode shape and, since Equation 1 is a set of second order differential equations, λ_m being its squared modal frequency ω_m.

$$\lambda_m = \omega_m^2 \tag{3}$$

Rather than solving the full system EVP (Equation 2), CMS splits the system into r subsystems or *components*. Each component has N_r degrees of freedom (DOFs), which are a subset of the N DOFs of the FE model. In turn, the component DOFs are split into $N_{i,r}$ interior DOFs and $N_{c,r}$ coupling interface DOFs. The displacement $\boldsymbol{u}_r$ in each component reads

$$\boldsymbol{u}_r = \begin{bmatrix} \boldsymbol{u}_i \\ \boldsymbol{u}_c \end{bmatrix}_r \tag{4}$$

By means of a coordinate transformation $\boldsymbol{T}_r$, each component's displacement is posed in a component modal basis.

$$\boldsymbol{u}_r = \boldsymbol{T}_r \boldsymbol{q}_r = \boldsymbol{T}_r \begin{bmatrix} \boldsymbol{q}_s \\ \boldsymbol{q}_c \end{bmatrix}_r \tag{5}$$

where $\boldsymbol{q}_{s,r}$ and $\boldsymbol{q}_{c,r}$ correspond to the interior and coupling DOFs respectively. The basis consists of $N_{s,r}$ *local* modes of the component. If all modes are used to create the basis the transformation in Equation 5 is exact. However, if the basis is truncated up to a smaller number of local modes the transformation is an approximation that will give no significant error in the frequency range below the highest kept modes. In this way model reduction is achieved. The components' mass and stiffness matrices are transformed as well, i.e.

$$\boldsymbol{K}_r^q = \boldsymbol{T}_r^T \boldsymbol{K}_r \boldsymbol{T}_r \; ; \; \boldsymbol{M}_r^q = \boldsymbol{T}_r^T \boldsymbol{M}_r \boldsymbol{T}_r \tag{6}$$

The components' transformed response and matrices are later assembled together imposing continuity in the coupling interfaces. This yields a full system reduced response q, and reduced mass $\boldsymbol{M}^q$ and stiffness $\boldsymbol{K}^q$ matrices. Hence, the equations of motion (Equation 1) can be posed in terms of the reduced basis, and the modal analysis is performed by solving a reduced EVP

$$\boldsymbol{K}^q \phi^q = \lambda \boldsymbol{M}^q \phi^q \tag{7}$$

where the original mode shapes are recovered by using the transformation $\phi = \boldsymbol{T}\phi^q$.

4 Complex component mode synthesis

Complex component mode synthesis (CCMS) considers the (viscously) damped equations of motion of the FE system.

$$\boldsymbol{M}\ddot{\boldsymbol{u}} + \boldsymbol{C}\dot{\boldsymbol{u}} + \boldsymbol{K}\boldsymbol{u} = \boldsymbol{f} \tag{8}$$

In order to perform modal analysis over the damped model the equations of motion have to be posed in state-space formulation.

$$\begin{bmatrix} \boldsymbol{0} & \boldsymbol{M} \\ \boldsymbol{M} & \boldsymbol{C} \end{bmatrix} \begin{bmatrix} \ddot{\boldsymbol{u}} \\ \dot{\boldsymbol{u}} \end{bmatrix} + \begin{bmatrix} -\boldsymbol{M} & \boldsymbol{0} \\ \boldsymbol{0} & \boldsymbol{K} \end{bmatrix} \begin{bmatrix} \dot{\boldsymbol{u}} \\ \boldsymbol{u} \end{bmatrix} = \begin{bmatrix} \boldsymbol{0} \\ \boldsymbol{f} \end{bmatrix} \tag{9}$$

Equation 9 can be rewritten by introducing the state-space response vector $\boldsymbol{x}$ consisting of the velocity $\dot{\boldsymbol{u}}$ and displacement $\boldsymbol{u}$ vectors of the FE model.

$$\boldsymbol{A}\dot{\boldsymbol{x}} + \boldsymbol{B}\boldsymbol{x} = \boldsymbol{f}^x \tag{10}$$

In this way, an EVP in state-space form can be solved in order to find the system modes.

$$\boldsymbol{B}\bar{\phi}^x = \bar{\lambda}\boldsymbol{A}\bar{\phi}^x \tag{11}$$

The solutions of this EVP are the complex eigenvalues $\bar{\lambda}_m$ and complex eigenvectors $\bar{\phi}^x_m$. Here the bar indicates that they are complex numbers. Due to the fact that state-space formulation has been introduced, the number of degrees of freedom N doubles with respect to the EVP for undamped modal analysis (Equation 2). Hence, the number of modal solutions N_m is also doubled. Since Equation 10 is a set of first order differential equations, the eigenvectors correspond to the system modal frequencies

$$\bar{\lambda}_m = -i\bar{\omega}_m \tag{12}$$

and they come in complex conjugate pairs $\bar{\lambda}_m$ and $\bar{\lambda}^*_m$, given that $\boldsymbol{A}$ and $\boldsymbol{B}$ are Hermitian matrices. The eigenvectors come in complex conjugate pairs as well, and they consist of the displacement mode shapes $\bar{\phi}_m$ and velocity mode shapes $\bar{\theta}_m$.

$$\bar{\phi}^x_m = \begin{bmatrix} \bar{\theta}_m \\ \bar{\phi}_m \end{bmatrix} \quad ; \quad \theta = \dot{\phi} \tag{13}$$

Analogously to classical CMS, component sub-structuring, component modal basis transformation ($\boldsymbol{x} = \bar{\boldsymbol{T}}^x \boldsymbol{q}^x$), and model order reduction can be defined for the state-space EVP, so that a reduced complex EVP is obtained.

$$\bar{\boldsymbol{B}}^{q^x} \bar{\phi}^{q^x} = \bar{\lambda}\bar{\boldsymbol{A}}^{q^x} \bar{\phi}^{q^x} \tag{14}$$

4.1 Complex component mode synthesis with fixed interface complex modes

One possible CCMS method is the one defined in [9], which is the direct extension to CCMS of the classical Craig-Bampton free interface CMS. For the purpose of this paper, it is convenient to use a fixed interface counterpart of this method. Therefore, the fixed interface CMS direct extension to CCMS is presented next.

Following the sub-structuring notation introduced in section 3, the state-space response vector for each component reads

$$\boldsymbol{x}_r = \begin{bmatrix} \dot{\boldsymbol{u}} \\ \boldsymbol{u} \end{bmatrix}_r \; ; \; \boldsymbol{x}_{i,r} = \begin{bmatrix} \dot{\boldsymbol{u}}_i \\ \boldsymbol{u}_i \end{bmatrix}_r \; ; \; \boldsymbol{x}_{c,r} = \begin{bmatrix} \dot{\boldsymbol{u}}_c \\ \boldsymbol{u}_c \end{bmatrix}_r \tag{15}$$

Then, the component response $\boldsymbol{x}_r$ can be expressed in terms of a fixed interface complex modes basis.

$$\boldsymbol{x}_r = \bar{\boldsymbol{T}}_r^x \boldsymbol{q}_r^x \quad ; \quad \boldsymbol{q}_r^x = \begin{bmatrix} \boldsymbol{q}_s^x \\ \boldsymbol{x}_c \end{bmatrix}_r = \begin{bmatrix} \boldsymbol{q}_s^x \\ \dot{\boldsymbol{u}}_c \\ \boldsymbol{u}_c \end{bmatrix}_r \tag{16}$$

The interior DOFs transformed response $\boldsymbol{q}_{s,r}^x$ is expressed in terms of the fixed interface complex modes. The coupling interface DOFs response $\boldsymbol{x}_{c,r}$ remain being the physical velocity $\dot{\boldsymbol{u}}_c$ and displacement $\boldsymbol{u}_c$ vectors.

The complex transformation matrix consists of two state-space sub-matrices, the fixed interface mode shapes matrix $\bar{\boldsymbol{\Phi}}_r^x$, and the constraint modes matrix $\boldsymbol{\Psi}_r^x$. The state-space fixed interface modes are computed by solving the state-space EVP for the component interior DOFs.

$$\boldsymbol{B}_{ii,r} \bar{\phi}_{i,r}^x = \bar{\lambda}_r \boldsymbol{A}_{ii,r} \bar{\phi}_{i,r}^x \tag{17}$$

The state-space constraint modes are analogous to the the ones used in Craig-Bampton fixed interface CMS, $\boldsymbol{\Psi}_{ic,r} = -\boldsymbol{K}_{ii,r}^{-1} \boldsymbol{K}_{ic,r}$. This happens because the static constraint relation holds for the velocity DOFs as it does for the displacement DOFs.

$$\boldsymbol{u}_r = \begin{bmatrix} \boldsymbol{\Psi}_{ic} \\ \boldsymbol{I}_{cc} \end{bmatrix}_r \boldsymbol{u}_{c,r} \quad ; \quad \dot{\boldsymbol{u}}_r = \begin{bmatrix} \boldsymbol{\Psi}_{ic} \\ \boldsymbol{I}_{cc} \end{bmatrix}_r \dot{\boldsymbol{u}}_{c,r} \tag{18}$$

Thus, the complex modes transformation matrix reads

$$\bar{\boldsymbol{T}}_r^x = \begin{bmatrix} \bar{\boldsymbol{\Phi}}_r^x & \boldsymbol{\Psi}_r^x \end{bmatrix} = \begin{bmatrix} \bar{\boldsymbol{\Theta}}_{is} & \boldsymbol{\Psi}_{ic} & \boldsymbol{0}_{ic} \\ \boldsymbol{0}_{cs} & \boldsymbol{I}_{cc} & \boldsymbol{0}_{cc} \\ \bar{\boldsymbol{\Phi}}_{is} & \boldsymbol{0}_{ic} & \boldsymbol{\Psi}_{ic} \\ \boldsymbol{0}_{cs} & \boldsymbol{0}_{cc} & \boldsymbol{I}_{cc} \end{bmatrix}_r \tag{19}$$

and, assuming $\bar{\boldsymbol{\Phi}}_r^x$ to be $\boldsymbol{A}_r$ normalised, the component transformed matrices show the same structure as for undamped fixed interface CMS

$$\bar{\boldsymbol{B}}_r^{q^x} = \begin{bmatrix} \bar{\boldsymbol{\Lambda}}_{ss} & \bar{\boldsymbol{B}}_{sc}^{q^x} \\ \bar{\boldsymbol{B}}_{cs}^{q^x} & \boldsymbol{B}_{cc}^{q^x} \end{bmatrix}_r \quad ; \quad \bar{\boldsymbol{A}}_r^{q^x} = \begin{bmatrix} \boldsymbol{I}_{ss} & \bar{\boldsymbol{A}}_{sc}^{q^x} \\ \bar{\boldsymbol{A}}_{cs}^{q^x} & \boldsymbol{A}_{cc}^{q^x} \end{bmatrix}_r \tag{20}$$

with $\bar{\boldsymbol{\Lambda}}_{ss,r}$ a diagonal matrix containing the complex fixed interface eigenvalues $\bar{\lambda}_{s,r}$, and $\boldsymbol{I}_{ss,r}$ an identity matrix of the same size.

Finally, conveniently arranging together the interior modal responses $q_t^x = \bigcup_r q_{s,r}^x$ and the coupling responses $x_c = \bigcup_r x_{c,r}$, so that

$$\boldsymbol{q}^x = \begin{bmatrix} \boldsymbol{q}_t^x \\ \boldsymbol{x}_c \end{bmatrix} \tag{21}$$

the full system transformed matrices are obtained by assembly of the component transformed matrices.

$$\bar{\boldsymbol{B}}^{q^x} = \begin{bmatrix} \bar{\boldsymbol{\Lambda}}_{tt} & \bar{\boldsymbol{B}}_{tc}^{q^x} \\ \bar{\boldsymbol{B}}_{ct}^{q^x} & \sum_r \boldsymbol{B}_{cc,r}^{q^x} \end{bmatrix} \quad ; \quad \bar{\boldsymbol{A}}^{q^x} = \begin{bmatrix} \boldsymbol{I}_{tt} & \bar{\boldsymbol{A}}_{tc}^{q^x} \\ \bar{\boldsymbol{A}}_{ct}^{q^x} & \sum_r \boldsymbol{A}_{cc,r}^{q^x} \end{bmatrix} \tag{22}$$

5 Local modal perturbational method

The LMP method [4] is a method that estimates the statistics of frequency response functions of a system at small computational cost. In LMP the system is divided into CMS components and the uncertainty in each component is assumed to be uncorrelated from the uncertainty in other components. Then, the uncertainty in each component is quantified in terms of the local modal properties of the component. Then, the uncertainty in the component modes is propagated to the full system modes based on Fox and Kapoor's formulation [6].

Fox and Kapoor's expressions describe the sensitivity of undamped modal frequencies and mode shapes of the full system to the variation in a physical parameter μ. For example, the linear expression for the m'th eigenvalue relates the perturbation $\delta\lambda_m$ in the eigenvalue due to a perturbation $\delta\mu$ in the physical parameter

$$\delta\lambda_m = \boldsymbol{\phi}_m^T \left[\frac{\partial \boldsymbol{K}}{\partial \mu} - \lambda_m \frac{\partial \boldsymbol{M}}{\partial \mu} \right] \boldsymbol{\phi}_m \delta\mu \tag{23}$$

and it follows from the partial derivative of Equation 2 with respect to the parameter μ, with $\boldsymbol{\phi}_m$ being $\boldsymbol{M}$ normalised. If this expression is posed in terms of the CMS formulation, the perturbation of the m'th *global* eigenvalue due to perturbation in the t'th *local* eigenvalue can be described

$$\delta\lambda_m = \boldsymbol{\phi}_m^{q^T} \left[\frac{\partial \boldsymbol{K}^q}{\partial \lambda_t} - \lambda_m \frac{\partial \boldsymbol{M}^q}{\partial \lambda_t} \right] \boldsymbol{\phi}_m^q \delta\lambda_t \tag{24}$$

where $\lambda_t = \lambda_{s,r}$.

Now, for simplicity, assume that uncertainty is only present in the component modal frequencies, i.e. components have deterministic mode shapes and coupling interfaces. Examining the system's mass and stiffness matrices in fixed interface Craig-Bampton form

$$\boldsymbol{K}^q = \begin{bmatrix} \boldsymbol{\Lambda}_{tt} & \boldsymbol{0} \\ \boldsymbol{0} & \sum_r \boldsymbol{K}_{cc,r}^q \end{bmatrix} \quad ; \quad \boldsymbol{M}^q = \begin{bmatrix} \boldsymbol{I}_{tt} & \boldsymbol{M}_{tc}^q \\ \boldsymbol{M}_{ct}^q & \sum_r \boldsymbol{M}_{cc,r}^q \end{bmatrix} \tag{25}$$

only the eigenvalues sub-matrix $\boldsymbol{\Lambda}_{tt}$ depends on λ_t under the assumptions above. Hence, all other sub-matrices derivatives $\frac{\partial}{\partial \lambda_t}$ in Equation 24 equal zero. Furthermore, since local eigenvalues are independent one to another, Equation 24 reduces to a simple perturbation relationship.

$$\delta\lambda_m = \left(\phi_{mt}^q\right)^2 \delta\lambda_t \tag{26}$$

If all component local eigenvalues are perturbed, the total perturbation in the m'th global eigenvalue is given by

$$\delta\lambda_m = \sum_t \left(\phi_{mt}^q\right)^2 \delta\lambda_t \tag{27}$$

Proceeding analogously, a similar relationship for the perturbation of global mode shape vectors due to perturbations in local eigenvalues can be found from the respective Fox and Kapoor's linear expression.

$$\delta\boldsymbol{\phi}_m^q = \sum_t \left(\sum_{n \neq m} \frac{\phi_{mt}^q \phi_{nt}^q}{\lambda_m - \lambda_n} \boldsymbol{\phi}_n^q \right) \delta\lambda_t \tag{28}$$

6 Complex local modal perturbational method

In this section, the direct extension of the LMP method to CCMS is presented. In the same way the rate of change of eigenvalues (Equation 23) is obtained from the derivation of the EVP in Equation 1 with respect to μ, the rate of change in CMS form (Equation 24) is derived from the derivation of the CMS-EVP in Equation 7 with respect to λ_t. Therefore, it is apparent that, by deriving the state-space EVP in Equation 14 with respect to $\bar{\lambda}_t$, an analogous expression for CCMS is obtained.

$$\delta\bar{\lambda}_m = \left[\bar{\boldsymbol{\phi}}_m^{q^x}\right]^T \left[\frac{\partial \bar{\boldsymbol{B}}^{q^x}}{\partial \bar{\lambda}_t} - \bar{\lambda}_m \frac{\partial \bar{\boldsymbol{A}}^{q^x}}{\partial \bar{\lambda}_t}\right] \bar{\boldsymbol{\phi}}_m^{q^x} \delta\bar{\lambda}_t \tag{29}$$

Using the fixed interface complex modes method presented in section 4.1, the state-space transformed matrices $\bar{\boldsymbol{B}}^{q^x}$ and $\bar{\boldsymbol{A}}^{q^x}$ show the same characteristics as the transformed mass and stiffness matrices in the undamped LMP method (cf. Equations 22 and 25). Therefore, under the assumptions considered in the LMP method a simple perturbation relationship is derived for complex eigenvalues.

$$\delta\bar{\lambda}_m = \left(\bar{\phi}_{mt}^{q^x}\right)^2 \delta\bar{\lambda}_t \tag{30}$$

Notice that complex conjugate eigenvalue pairs in $\bar{\boldsymbol{\Lambda}}_{tt}$ are also independent since for any complex number $z \in \mathbb{C}$ the partial derivative of the complex conjugate function is zero, $\frac{\partial z^*}{\partial z} = 0$.

Thus, the complex local modal perturbational method uses the simple perturbation relationships for the system's complex eigenvalues and eigenvectors

$$\delta\bar{\lambda}_m = \sum_t \left(\bar{\phi}_{mt}^{q^x}\right)^2 \delta\bar{\lambda}_t \tag{31}$$

$$\delta\bar{\boldsymbol{\phi}}_m^{q^x} = \sum_t \left(\sum_{n \neq m} \frac{\bar{\phi}_{mt}^{q^x} \bar{\phi}_{nt}^{q^x}}{\bar{\lambda}_m - \bar{\lambda}_n} \bar{\boldsymbol{\phi}}_n^{q^x} \right) \delta\bar{\lambda}_t \tag{32}$$

to compute the statistics of the frequency response functions of the system.

6.1 Perturbation of local modal frequencies

A significant difference between the undamped and the damped LMP methods is that the local eigenvalues λ_t and $\bar{\lambda}_t$ do not represent the same physical quantity. (cf. Equations 3 and 12). A damped modal frequency $\bar{\omega}_t$ is determined by the corresponding undamped modal frequency ω_t and modal damping factor η_t. If the uncertainty in the ω_t and η_t parameters is assumed to be independent, these parameters might be perturbed independently, i.e. $\delta\omega_t$ and $\delta\eta_t$, in order to perturb the complex damped eigenvalues, i.e.

$$\delta\bar{\lambda}_t = \bar{\lambda}_t\left(\omega_t + \delta\omega_t, \eta_t + \delta\eta_t\right) - \bar{\lambda}_t\left(\omega_t, \eta_t\right) \tag{33}$$

For example, for viscously damped components the ω_t and η_t parameters can be obtained directly from the nominal local eigenvalues

$$\omega_t = \left|\bar{\lambda}_t\right| \;\; ; \;\; \eta_t = -2\frac{\mathrm{Re}\left\{\bar{\lambda}_t\right\}}{\left|\bar{\lambda}_t\right|} \tag{34}$$

so that independent perturbations can be applied to both parameters, from which the perturbed eigenvalues follow.

$$\bar{\lambda}_t = -\omega_t\left(\frac{\eta_t}{2}\right) - i\omega_t\sqrt{1 - \left(\frac{\eta_t}{2}\right)^2} \tag{35}$$

7 Numerical Example

The complex LMP (CLMP) method is illustrated in this section through a numerical example. The CLMP method has been executed over the Z-shaped structure presented in Figure 1. The structure consist of three aluminium tubes with rectangular cross section. The Z-shaped structure is simply supported at the end-openings bottom corners. The physical properties of the structure are resumed in Table 1.

Damping is chosen to be of viscous kind. The tubes are mass and stiffness proportionally damped, i.e. $C = \alpha M + \beta K$, with the proportionality constants chosen so that the system is very lightly damped (modal damping values below 0.1% in the mid-frequency range). Additionally, a point viscous damper (c_1, c_2, c_3) is applied to each of the tube sections as shown in Figure 1, so that the overall damping is increased and the structure becomes non-classically damped.

The Z-shaped structure is assumed to be deterministic, except for the point viscous dampers which present some uncertainty. Their damping value has a gaussian probability distribution function centered at the dampers' nominal value and with a relative standard deviation of 5% times the nominal value.

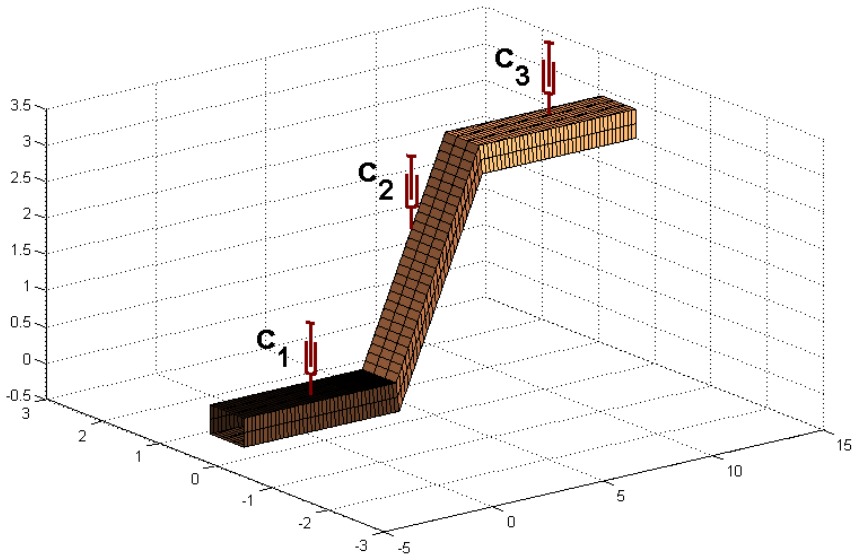

Figure 1: Z-shaped structure with 3 point dampers.

Parameter	Value	Units
Elastic Modulus	$2.11 \cdot 10^{11}$	N/m^2
Poisson Ratio	0.3	
Shear Modulus	$8.071 \cdot 10^{10}$	N/m^2
Density	7800	kg/m^3
Cross Section	0.04×0.06	m^2
Length	$l_1 = l_3 = 0.7, l_2 = 0.5$	m
Damping Factors	$\alpha = 20$	s^{-1}
	$\beta = 4 \cdot 10^{-6}$	s
	$c_1 = c_2 = c_3 = 0.1$	kg/s

Table 1: Physical parameters of the Z-shaped structure and lumped dampers.

7.1 Simulation description

The numerical simulation involved the following steps.

The structure's FE model has been meshed using 1050 shell elements. Three substructures have been defined corresponding to each of the tubes with local damper, giving rise to three components with 4800, 3360 and 4800 state-space degrees of freedom respectively.

Modal analysis has been performed using complex component mode synthesis as described in Section 4. The first 100 fixed-interface complex modes (50 mode pairs) have been computed for each component (Equation 17), so that the FE model is transformed into CCMS coordinates. The reduced model has 300 local modal degrees of freedom and 240 state-space coupling degrees of freedom. Then, the global eigenvalue problem in CCMS coordinates (Equation 14) is solved to obtain the first 200 complex modes (100 mode pairs) of the full structure.

Uncertainty analysis has been performed through Monte Carlo simulation. The statistics of the modal solution have been computed using 100 Monte Carlo samples. For each sample the fixed-interface complex modal frequencies have been perturbed according to the damping uncertainty of the point dampers. Then, the perturbation has been propagated to full system complex modal frequencies following Equation 31. No perturbation of system's modal vectors have been considered in this simulation. From the MC simulation, the frequency and damping statistics of the components' fixed-interface and the full structure complex modes have been computed.

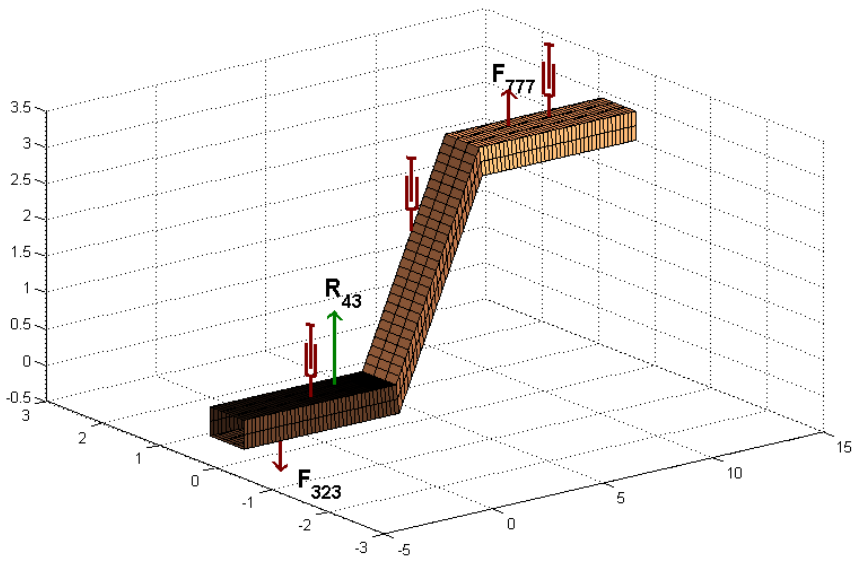

Figure 2: Forces and Response points defined over the structure with 3 lumped dampers.

Finally, point harmonic forces have been applied to the structure as shown in Figure 2 at mesh nodes 323 and 777. The velocity response (from 0 Hz to 2 kHz) at node 43 has been computed through modal summation for all MC samples, from which the mean and extreme responses have been derived.

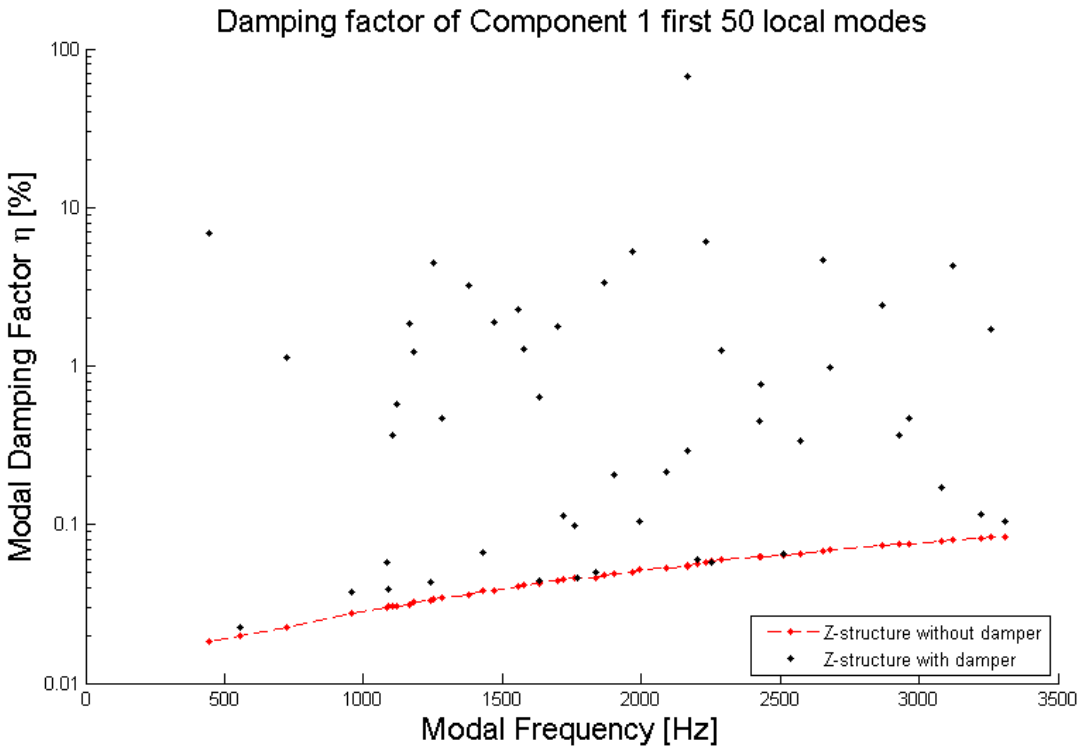

Figure 3: Modal damping of Component 1 fixed-interface local modes. Red - System without point dampers. Black - System with point dampers.

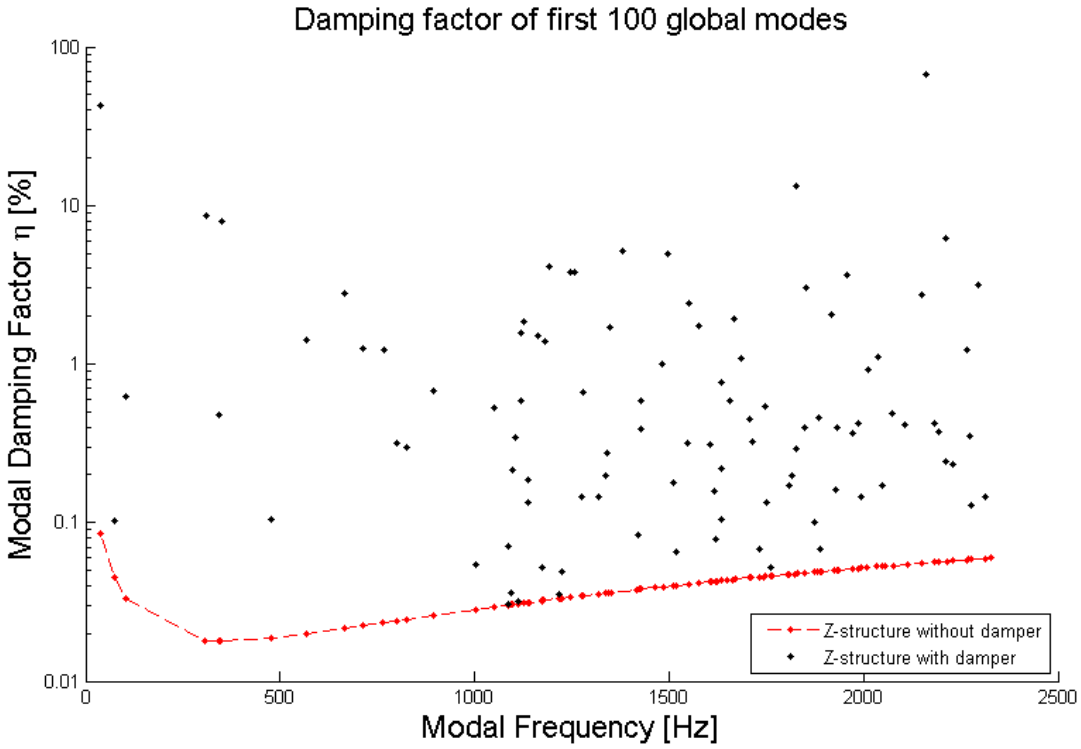

Figure 4: Modal damping of full system modes. Red - System without point dampers. Black - System with point dampers.

7.2 Results

The effect of adding localized damping in the nominal structure is first evaluated. In order to do so, a comparison of the modal solutions for two different cases is performed. The two cases are the Z-shape structure without the point viscous dampers, and the Z-shape structure with the point viscous dampers.

In Figure 3 the modal damping values of the fixed-interface modes of Component 1 are shown for the two cases. The modes locii in a frequency-damping coordinates system is plotted in red dots for the case without dampers, and in black dots for the case with dampers. For the case without dampers the system is proportionally damped, and the modes' damping follows the typical stiffness controlled proportional damping curve. On the contrary, when local damping is introduced the added damping gets unevenly distributed among the different component modes depending on the mode shape amplitude of each mode at the placement of the point damper. Some modes get highly damped, whereas others get almost no extra damping, and their damping value remain close to the proportional damping values. For this reason the black dots get scattered, making it apparent that the proportional damping assumption is far inappropriate for systems with localised damping. Similar plots to the one in Figure 3 are obtained for Components 2 and 3.

In Figure 4 the modal damping values of the system global modes are shown for the two same cases. For the case without dampers the values follow again the proportional damping curve, mass controlled below 300 Hz, stiffness controlled over 500 Hz. When local damping is introduced instead, the global modes get also unevenly damped since they are a weighted combination of the local modes of the three components.

Next, the results of the Monte Carlo simulation are evaluated. The CLMP method has been applied to the non-classically damped case. The perturbation of fixed-interface complex frequencies is defined in the following way.

Only the point dampers present uncertainty. Therefore the frequencies perturbation depends only on the randomness of the point dampers. Hence, the damping $\Delta\eta_s^r$ added by the point damper c_r to the sth mode of component r is obtained by subtracting the proportional modal damping $\eta_{s,ref}^r$ (red curve in Figure 3) to the overall damping η_s^r (black dots in Figure 3):

$$\Delta\eta_s^r = \eta_s^r - \eta_{s,ref}^r \tag{36}$$

The uncertainty in the point damper perturbs only the added damping $\Delta\eta_s^r$. Thus the perturbation in components' modal damping may be computed as:

$$\eta_{s,pert}^r = \eta_{s,ref}^r + \Delta\eta_s^r \left(1 + \epsilon^r\right) \tag{37}$$

with ϵ^r a sample of a gaussian random variable with zero mean and standard deviation $\sigma^r = 0.05$, which is the relative standard deviation of the point dampers. Finally,the perturbation in component complex modal frequencies is computed following Equation 33, and the perturbation is propagated to global modes using the CLMP expressions.

Figure 5 shows the modal damping relative standard deviation σ_{η_s} of the local modes in Component 1. The relative standard deviation has been computed from the 100 perturbation samples of the Monte Carlo simulation. Additionally, the absolute modal damping of the nominal model is indicated with red dots. It can be observed that those modes that get highly damped by the point damper have a standard deviation close to 5% of the point damper. Modes that get almost no damping increase with respect to the proportionally damped case show consequently small relative standard deviation.

Figure 6 shows the modal damping relative standard deviation σ_{η_m} of the full system modal modes. Due to the non-proportional nature of the system damping, the global modes get perturbed in a significantly uneven manner. Some global modes are very sensitive to the local damping perturbation (40% to 60% damping relative STD). This modes happen to be modes which are still lightly damped (damping below 1%). This may happen because the major contributions to their damping, althouh small, come from component local modes that have high damping perturbation. Conversely, highly damped global modes end up having small relative standard deviation, and they may not exceed the standard deviation of the point dampers.

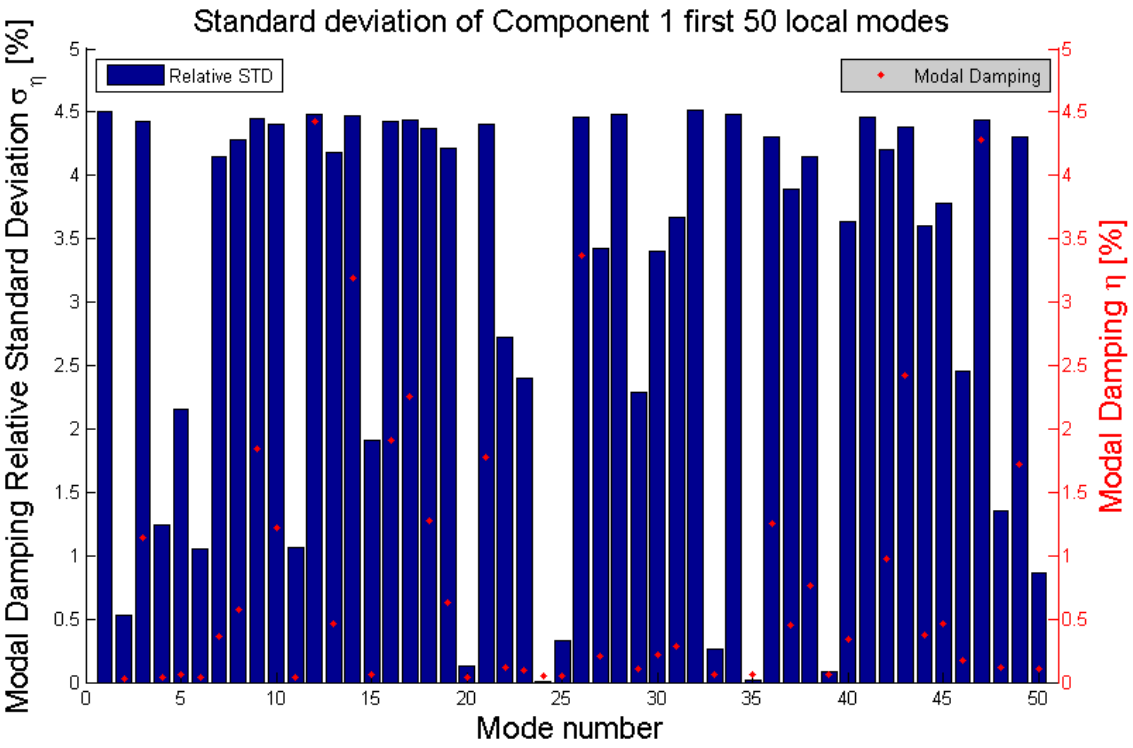

Figure 5: Modal damping of the local modes in Component 1. Blue bars - Relative standard deviation. Red dots - Nominal value.

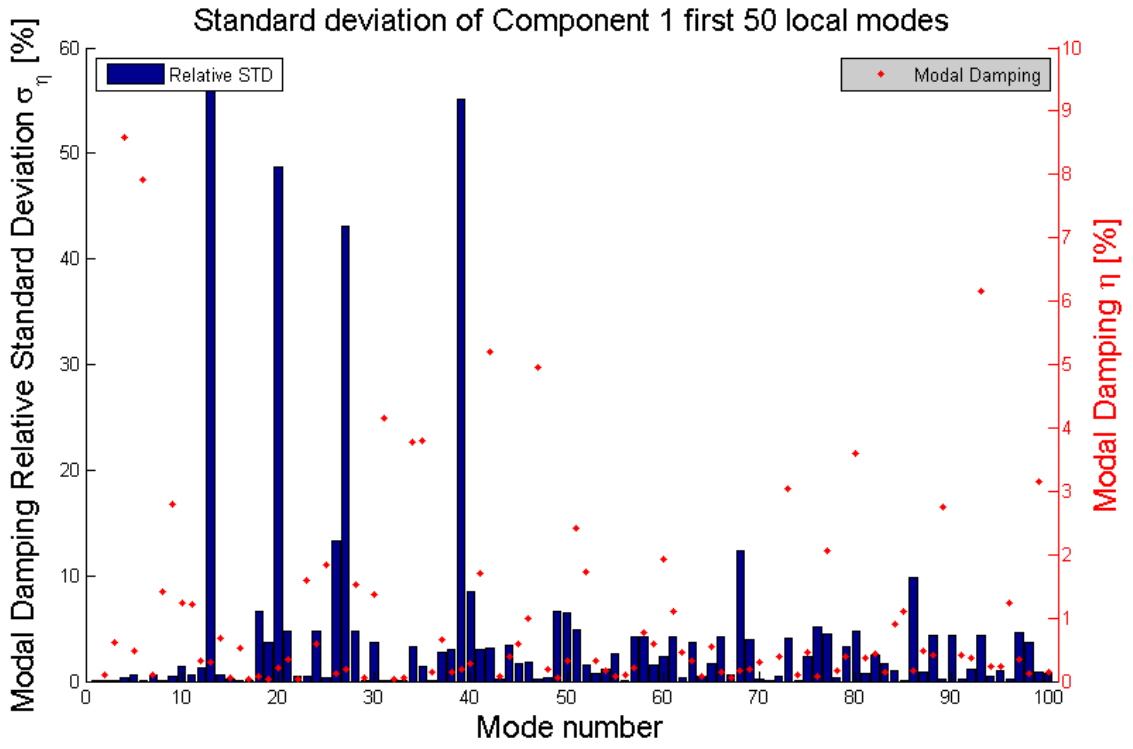

Figure 6: Modal damping of the full system modal modes. Blue bars - Relative standard deviation. Red dots - Nominal value.

It is important to notice that the uncertainty in the point dampers induces large variation in lightly damped modes. This means that the peaks levels of the structure's frequency response functions present significant uncertainty. Figure 7 shows the velocity response function with the forcing and response points as defined in Figure 2. It can be observed that three of the peaks present large variation. These peaks correspond to the four modes that show larger relative standard deviation (the second peak containing two of them). The CLMP method makes it possible to estimate this damping uncertainty in the response functions.

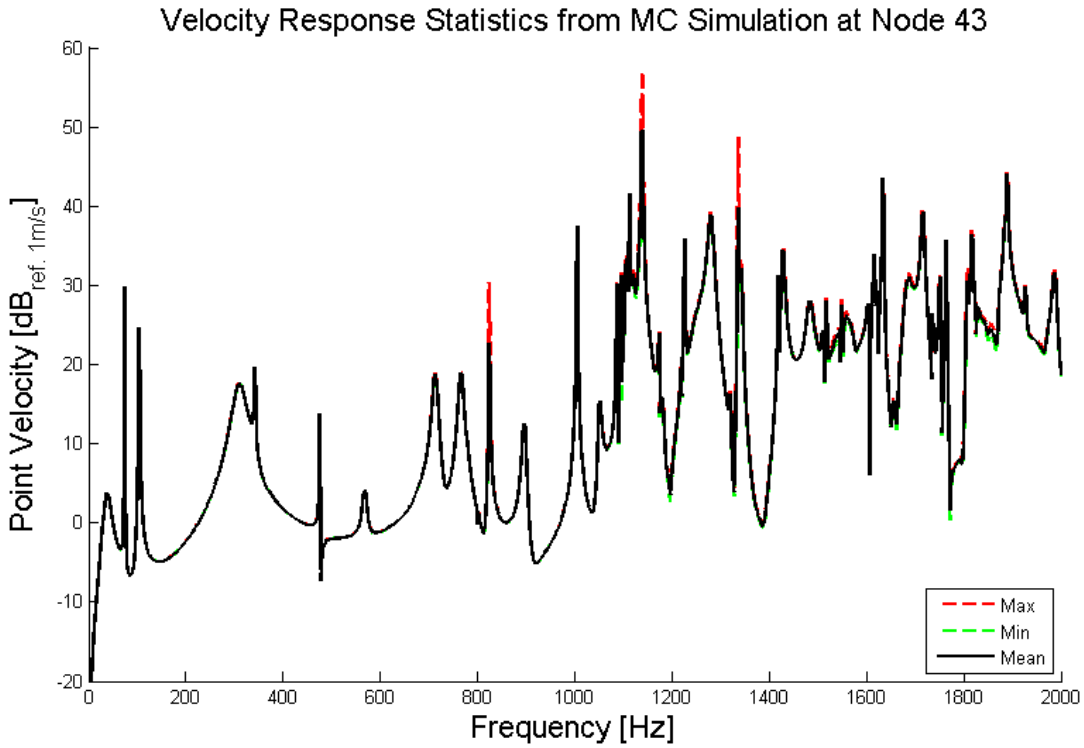

Figure 7: Velocity response of the Z-shaped structure with 3 lumped dampers at node 43. Black line - Mean response. Green dashed line - Minimum response. Red dashed line - Maximum response.

For the present simulation, the total time for perturbing component modes and propagating the uncertainty to global modes for the 100 Monte Carlo samples was 2.86 s. In contrast, for solving once the FE model, the components' state-space EVP solving time was 14.46s, 13.19s and 14.56s for Component 1, 2 and 3 respectively. The global CCMS EVP solving time was 9.16s. Thus, using the CLMP method, the CCMS modal analysis has to be performed only once, and the subsequent 99 Monte Carlo samples are obtained at a negligible computational cost compared to solving 99 times the CCMS modal analysis.

8 Conclusions

A new perturbation method for SFEM based on complex component mode synthesis has been presented. The method is an extension of the local modal perturbational method for non-classically damped systems. As in the LMP method, the computational gain comes from the fact that the nominal FE model of the system has to be solved only once, and all other Monte Carlo samples are computed using the computationally cheap modal perturbation relationships. Introduction of the state-space formulation makes it possible to treat damping at a component level. This is done at the price of doubling the number of degrees of freedom of the EVP to solve. The computation time for propagating the perturbations is also increased with respect to undamped LMP, since complex LMP presents twice as many eigenvalues and these are complex valued. Nevertheless, the overall computation time is several orders of magnitude lower than performing a full system solving Monte Carlo simulation.

9 Acknowledgements

The authors gratefully acknowledge the ITN Marie Curie project GA-214909 "MID-FREQUENCY - CAE Methodologies for Mid-Frequency Analysis in Vibration and Acoustics".

References

[1] L. Hinke, B. R. Mace, F. Dohnal, T. P. Waters, and N. S. Ferguson. Component mode synthesis as a framework for uncertainty analysis. *Journal of Sound and Vibration*, 324:161–178, 2009.

[2] W.C. Hurty. Dynamic analysis of structural systems using component modes. *AIAA Journal*, 3:678–685, 1965.

[3] R.R. Craig and M. Bampton. Coupling of substructures for dynamic analysis. *AIAA Journal*, 6:1313–1319, 1968.

[4] B.R. Mace and P.J. Shorter. A local modal/perturbational method for estimating frequency response statistics of built-up structures with uncertain parameters. *Journal of Sound and Vibration*, 242:793–811, 2001.

[5] S.N. Voormeeren, D. de Klerk, and D.J. Rixen. Uncertainty quantification in experimental frequency based substructuring. *Mechanical Systems and Signal Processing*, 24:106–118, 2010.

[6] R. L. Fox and M. P. Kapoor. Rates of change of eigenvalues and eigenvectors. *AIAA Journal*, 6:2426–2429, 1968.

[7] R.R. Craig and Z. Ni. Component mode synthesis for model order reduction of nonclassically damped systems. *AIAA Journal of Guidance, Control, and Dynamics*, 12:577–584, 1989.

[8] W. Wang and J. Kirkhope. Complex component mode synthesis. *Journal of Sound and Vibration*, 181:781–800, 1995.

[9] J. A. Morgan, C. Pierre, and G. M. Hulbert. Baseband methods of component mode synthesis for non-proportionally damped systems. *Mechanical Systems and Signal Processing*, 17:589–598, 2003.

[10] S. Adhikari. Rates of change of eigenvalues and eigenvectors in damped dynamic systems. *AIAA Journal*, 39:1452–1457, 1999.

[11] Q. H. Tran, M. Ouisse, and N. Bouhaddi. A robust component mode synthesis method for stochastic damped vibroacoustics. *Mechanical Systems and Signal Processing*, 24:161–181, 2010.